



TECHNICAL UNIVERSITY OF CLUJ-NAPOCA

ACTA TECHNICA NAPOCENSIS

Series: Applied Mathematics, Mechanics, and Engineering
Vol. XX, Issue xx, Month, 20xx

COMPLEX THERMO-MECHANICAL ANALYSIS OF EXTERNALLY DRIVEN MAIN SPINDLES – A CASE STUDY

George CONSTANTIN, Constantin DOGARIU, Claudiu-Florinel BÎȘU,
Andrei GHEORGHITĂ, Dragoș AROTĂRIȚEI, Ionuț Gabriel GHIONEA

Abstract: The article treats a main spindle-bearing assembly that operates at high speeds from the perspective of complex modeling. The simulation of the dynamic and thermo-mechanical behavior is considered. Some important contributions are highlighted regarding the complex simulation of the main spindle. Mathematical modeling of heat generation in radial-axial angular contact ball bearings is treated. The heat generated is considered the source in the FEM models. The article approaches a case study of the main spindle of a milling machining center with speeds up to 9000 rpm. The experimental results regarding the temperatures of the bearings for various speeds with and without cooling of the casing and dynamic measurements are achieved. The CAD model of the main spindle studied is generated and imported into the FE program. Based on the mathematical model of the heat, the model is loaded with the bearings and belt drive heat sources and, as a result of the simulation, the overall temperatures is obtained. The situations without cooling (up to 4000 rpm) and with cooling 4000-8500 rpm are considered. The simulated values almost overlap with those measured, so that the model is validated. The thermal deformations for the cooled and non-cooled assembly are obtained by simulation. The natural frequencies are obtained by dynamic simulation and compared with the working ones. The conclusions emphasize an algorithm for experimental research combined with mathematical modeling and numerical analysis through FEA and specific aspects related to the functionality of the assembly.

Key words Main Spindle, Angular Contact Ball Bearing, Heat Transfer, Thermal Parameters, FEA.

1. INTRODUCTION

In the development of machine-tool type products or in their exploitation, design-research methods are used from the category of modeling and simulation, such as digital block simulation (DBS), finite element method (FEM) or rigid body simulation (RBS) [1] separately or combined. Each of individual methods is limited in estimating the behavior of the main spindle.

Therefore, all these components must be assembled so as to influence each other.

Currently, the simulation activities are separated from each other. Current research combines different types of simulation to capture different interdependencies, such as establishing frequency response with finite element analysis (FEA) combined with a simulation of the digital block model of the

machine tool [2]. Simulation of the deformation process has become almost usual in the industry, while simulation of cutting processes is an element of international research (this excludes the simulation of the NC program, which is widely used in the industry, but which does not reflect the actual behavior of the interaction between the machine tool, cutting tool and part during cutting operations).

A development process using virtual prototypes allows the designer to constantly analyze the kinematic, static and dynamic characteristics of the entire machine tool to find a constructive variant that meets the requirements. In the next few years, simulation technology will develop to a great extent and will be widely used in the design of innovative and competitive machine tools.

The model of a main spindle is based on variables that can be design variables and functional variables. These can be features of the main spindle and the bearings, arrangement of bearings, and also the axial preloading of the bearings [3].

The natural frequencies of a main spindle are influenced by its dimensions – lengths and diameters [4]. The values of the main spindle natural frequencies are increased with the diameter and decreased with the length. Additional mass on the rear of the main spindle improves the main spindle dynamics. The tool holder and cutting tool through their masses are greatly influencing the assembly behavior. Also the speed and loads in the process have a strong influence.

The bearings by their type, the material of the intermediate elements (balls, rollers) and their number influence the behavior of the bearings of the main shaft. The type of bearing assembly influences the rigidity of the main spindle-bearing assembly. The constructive elements – distance between the front and rear bearings and distances between the bearings and the free end of the tool – influence the first two modes of vibration of the assembly.

There is a direct proportional relationship between the axial preload of the bearing and the size of the natural frequencies of the spindle-bearings assembly. Basically, the rigidity of the assembly increases with the increase of the pretensioning [5]. Obviously, a higher rigidity caused by increased preload leads to better vibration behavior. Thus, the amplitude of the vibrations is reduced being accompanied by a reduction of the damping.

The operating parameters main spindle speed and temperature of bearings have a non-linear influence on the operation of the main spindle-bearing assembly.

Increasing the speed influences the rigidity of the bearings [6].

The dynamics of the system, more precisely the first natural frequencies, are changed by the speed of the shaft [7].

The temperature in the spindle bearings can influence the dynamics of the system. Therefore, the control of the temperature of the cooling fluid through a specific system leads to the control of the dynamic behavior of the system.

Spindle-bearing assembly has as main components the spindle and bearings along with many other components. The analysis of spindle-bearing assemblies is basically oriented to one of the following directions: mechanical deformations as result of loads (forces and moments), thermal analysis (thermal distribution on assembly, thermal deformations), vibrational behavior and modal analysis. The mechanic deformations of main spindles are usually calculated using theory of elasticity, Euler-Bernoulli or Timoshenko approximation [8, 9]. Most of the papers that deal with deformation of bearings (taking into account the lubricant) are based on [10]. The analysis of vibration is made usually for obtaining the natural frequencies [11]. There is also the possibility to record experimentally the spectrum of frequencies at constant rotation speed of spindle.

The heat sources are considered to be provided by the friction phenomenon in bearings, especially angular contact bearings used for high speeds [12–17]. A common approach to study the dynamic behavior of spindle-bearings assembly is FEM [18–20] based on CAD (computer-aided design) tools for design and thereafter the multiphysics modules from ANSYS, ABAQUS or SolidWorks. The amount of generated heat (produced by bearings), taking into account the friction models and contact model (usually the Hertz model), depend on many factors, such as contact angle, lubricant (grease in most of the cases), etc. [10, 21].

It is difficult to simulate the steady state temperature for a rotating spindle with bearings in FEM model. The usually way is to calculate the generation of heat for each bearing at a constant defined rotation speed (eventually an equal distribution between inner and outer rings), and to calculate the distribution of temperature, deformation, etc. considering the spindle bearings in a static position. In FE model, the contact stiffness between two bodies along with the characteristic of material for each part of the assembly must be provided.

Some article proposes alternatives to calculate the heat propagation using simplified geometries of spindle-bearings-housing and thermal networks [22, 23]. The thermal

resistance network can be very complicated. In order to build heat transfer equations, thermal resistance for each solid body according to its geometry should be calculated [23, 24]. The work [25] proposes one of the most used method for calculating thermal contact resistance between balls and rings. However, the thermal generators given by friction inside the bearings are calculated as in FEM model.

2. BEARING HEAT GENERATION

In literature, there are models including mathematical relations of variables (deformation, angular contact, forces and torques) in angular contact ball bearings under dynamic conditions as axial and radial loads, bearing preload starting with [10]. Other developments are based on these assumptions and are proposed by [26] and Antoine [27]. The current approach is based on [26].

The usually geometric dimensions for angular contact bearings used in calculus are: D – ball diameter; r_o – outer groove radius; r_i – inner groove radius; d_o – outer raceway diameter; d_i – inner raceway diameter; D_0 – ball diameter; and Z – number of balls. The relationship from Figs. 1–2 stands for a ball position angle ψ from vertical axis of the bearing with and without loads.

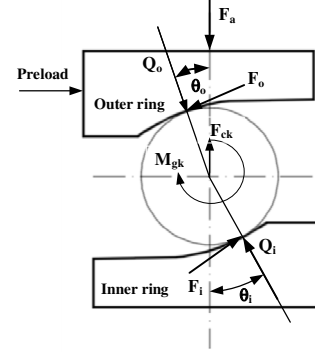


Fig. 1. Forces and moments in the assembly ball-rings.

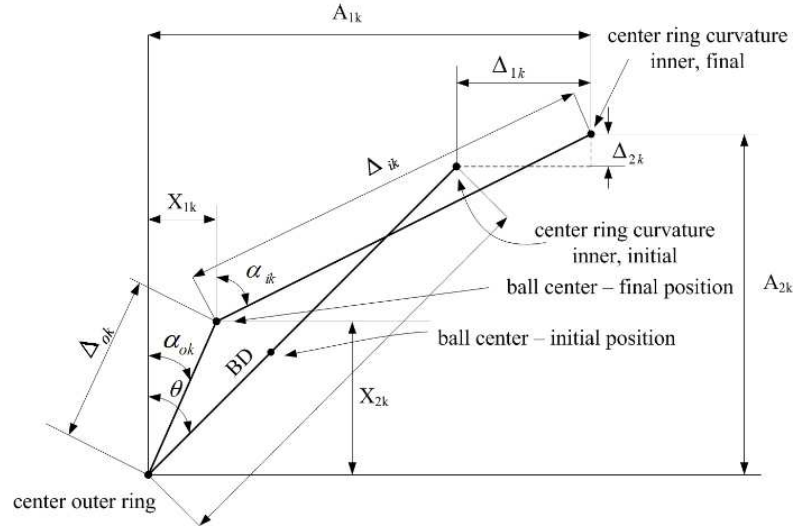


Fig. 2. Geometry in operation of ball-rings assembly.

The Hertz contact theory is used to model the contact force between the balls and the inner/outer ring (δ – ball deflection).

$$(A_{1k} - X_{1k})^2 + (A_{2k} - X_{2k})^2 - \Delta_{ik}^2 = 0, \quad (1)$$

$$X_{1k}^2 + X_{2k}^2 - \Delta_{ok}^2 = 0, \quad (2)$$

$$Q_{ok} \cos \alpha_{ok} - \frac{M_{gk}}{D} \sin \alpha_{ok} - Q_{ik} \cos \alpha_{ik} + \frac{M_{gk}}{D} \sin \alpha_{ik} - F_{ck} = 0, \quad (3)$$

$$Q_{ok} \sin \alpha_{ok} + \frac{M_{gk}}{D} \cos \alpha_{ok} - Q_{ik} \sin \alpha_{ik} - \frac{M_{gk}}{D} \cos \alpha_{ik} = 0. \quad (4)$$

The inter-dependencies from equations (1) – (4), are related by frequency of rotation of inner ring (or outer ring) fixed on the spindle are given shortly by (the bearing misalignment angle is neglected) [10]:

$$\Delta_{ik} = (f_i - 0.5)D + \delta_{ik}, \quad (5)$$

$$\Delta_{ok} = (f_o - 0.5)D + \delta_{ok}, \quad (6)$$

$$A_{1k} = BD \sin \alpha^0 + \delta_a, \quad (7)$$

$$A_{2k} = BD \sin \alpha^0 + \delta_r \cos \psi_k, \quad (8)$$

$$\cos \alpha_{ok} = X_{2k} / [(f_o - 0.5)D + \delta_{ok}], \quad (9)$$

$$\sin \alpha_{ok} = X_{1k} / [(f_0 - 0.5)D + \delta_{ok}], \quad (10)$$

$$\cos \alpha_{ik} = (A_{2k} - X_{2k}) / [(f_0 - 0.5)D + \delta_{ik}], \quad (11)$$

$$\sin \alpha_{ik} = (A_{1k} - X_{1k}) / [(f_0 - 0.5)D + \delta_{ik}], \quad (12)$$

$$F_{ck} = \frac{1}{2} m D \omega^2 \left(\frac{\omega_E}{\omega} \right)_k^2, \quad (13)$$

$$M_{gk} = J \omega^2 \left(\frac{\omega_b}{\omega} \right)_k \left(\frac{\omega_E}{\omega} \right)_k \sin \alpha_k, \quad (14)$$

$$Q_{ik} = K_i \delta_{ik}^{3/2}, \quad Q_{ok} = K_o \delta_{ok}^{3/2}, \quad (15)$$

$$\alpha_k = \tan^{-1}(\sin \alpha_{ik} / (\cos \alpha_{ik} - h)), \quad (16)$$

$$\left(\frac{\omega_E}{\omega} \right)_k = \frac{\cos(\alpha_{ik} - \alpha_{ok}) - h \cdot \cos \alpha_{ok}}{1 + \cos(\alpha_{ik} - \alpha_{ok})}, \quad (17)$$

$$\left(\frac{\omega_B}{\omega} \right)_k = \frac{1}{h \cos \alpha_k} \cdot \frac{-1}{\left(\frac{\cos \alpha_{ok} + \tan \alpha_k \sin \alpha_{ok}}{1 + h \cos \alpha_{ok}} + \frac{\cos \alpha_{ik} + \tan \alpha_k \sin \alpha_{ik}}{1 - h \cos \alpha_{ik}} \right)}. \quad (18)$$

In equations (5)–(18), α^0 is the initial contact angle (before loading) or free contact angle, R_i – radius to locus of raceway groove curvature centers, δ_a – relative axial displacement, δ_r – relative radial displacement, m – mass of ball, J – inertial moment (based on geometry of the body), F_{ck} – centrifugal forces, M_{gk} – gyroscopic moments on bearing ball, ω_m – orbital speed (rotating ball) in angular position ψ_k , ω_R – angular speed of the ball, F_{ik} and F_{ok} – forces given by gyroscopic moment, M_{gk} – gyroscopic moment of ball in k position, and k_i, k_o – stiffness of contact due to Hertz theory. The index notations are: r – radial and a – axial.

The *Newton-Raphson* numerical method is used in general to solve the equations (1)–(4) and the refinements proposed by [26] are used in this case.

The heat generated by the bearing speed of rotation n [rpm] is the additive formula for three friction torques: load friction torque, viscous friction torque, and spinning torque [10, 21, 28]. For steel material and Z number of balls, the total heat generated by the bearing with angular contact is given by (1.047×10^{-4} constant stands for steel):

$$H_f = Z \cdot (1.047 \times 10^{-4} \cdot n \cdot M_t), \quad (19)$$

$$M_t = M_l + M_v + M_s, \quad (20)$$

where:

$$M_l = f_1 F_\beta d_m, \quad (21)$$

$$M_v = \begin{cases} 10^{-7} f_0 (v_0 n)^{2/3} d_m^3 & \text{if } v_0 n \geq 2000 \\ 160 \times 10^{-7} f_0 d_m^3 & \text{if } v_0 n < 2000 \end{cases}, \quad (22)$$

$$M_s = \frac{3\mu Q_i a_i E_i}{8}. \quad (23)$$

The notations are similar to those in [28]: d_m – pitch diameter, v_0 – kinematic viscosity, n – spindle speed in rpm, f_0 – constant depending on bearing type and lubrication, $f_1 = z(P_0/C_0)^y$ (z, P_0 , and C_0 are calculated from tables), F_β – dynamical load, E_i – complete elliptic integral of second kind, a – major axis of deformation of ball modeled by an ellipse, and μ – friction coefficient.

The gyroscopic torque for each ball bearing in this location, even having a small value, at high speed rotation of the spindle is taken into account [10]:

$$M_g = \frac{1}{60} \cdot \rho \cdot \pi \cdot D^5 \cdot \omega_R \cdot \omega_m \cdot \sin \beta, \quad (24)$$

where ρ – density of material, ω_R – angular velocity of the ball around of its axis, ω_m – angular velocity of the ball, and β – angle between normal Z axis and axis of the ball.

For roller (cylindrical) bearing, in eq. (2) the spinning torque is null, meanwhile F_l takes into account the contact line between the roller and inner/outer raceway, so the friction will consider the length of cylinder L [29].

2. SPINDLE-BEARING ASSEMBLY EXPERIMENTAL MEASUREMENTS

The experimental measurements of the dynamic and thermal behavior were performed directly on the machine tool, after the spindle was subjected to a major repair. The experimental analysis aims to evaluate the dynamic and thermal parameters of the spindle. The vibration measurement of spindle is performed by using accelerometers fixed on the front and rear side of spindle (Fig. 3). The thermal behavior is achieved by a Fluke laser sensor without contact during axis rotation with a certain speed.

The machine tool is a Schaublin milling center, with 3 NC axes, BT40 tool holder and a maximum speed of 9000 rpm. The vibration signals were acquired using a multichannel equipment National Instruments USB4432, 24 bits resolutions, sampling rate 100 kS/s/ch and PCB, and Burel&Kjaer accelerometers with 100 mV/g sensitivity.

Signal processing and recording was done in real time.

Values of measured temperature and vibration parameters are given in Tables 1 and 2 and Figs. 4 and 5. From the measurements, it turns out



Fig. 3. Positions of sensors.

the vibration velocity for the main bearing $L1$ and rear one $L2$ (Fig. 6), and the acceleration level for evaluating the state of the bearings: front bearing – 0.51 g, and rear bearing – 0.58 g (Fig. 7). The frequency spectrum is shown in Fig. 8.

Table 1

Temperature monitoring.			
Speed n [rpm]	Front bearing T_1 [°C]	Rear bearing T_2 [°C]	Time [min]
1000	29	30	18.00
1500	29	31	18.30
2000	30	31	19.00
2500	30	32	19.30
3000	32	33	19.50
3500	33	36	20.30
4000	30	33	20.47
Cooling set on			
4500	29	30	21.15
5000	29	30	21.30
5500	29	20	21.55
6000	29	30	22.20
6500	29	20	22.40
7000	29	31	22.51
7500	29	31	22.22
8000	29	31	23.50
8500	29	31	24.25

Table 2

Vibration monitoring.				
Speed n [rpm]	L_1 [mm/s]	g	L_2 [mm/s]	g
1006	0.07	0.15	0.04	0.18
2012	0.14	0.28	0.08	0.36
3018	0.15	0.64	0.09	0.78
4025	0.14	0.35	0.15	0.79
5031	0.31	0.29	0.23	0.83
6042	0.23	0.49	0.21	0.84
7043	0.41	0.63	0.42	1.07
8049	0.47	0.54	0.54	1.22
8553	0.52	0.62	0.64	1.31

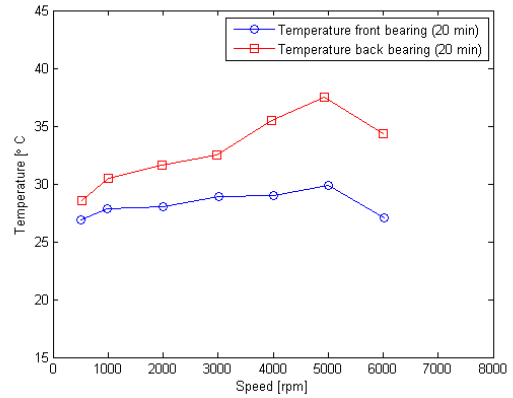


Fig. 4. Temperature (monitored), 6000 rpm, front bearing $T_{1max} = 30$ °C, back bearing $T_{2max} = 36$ °C.

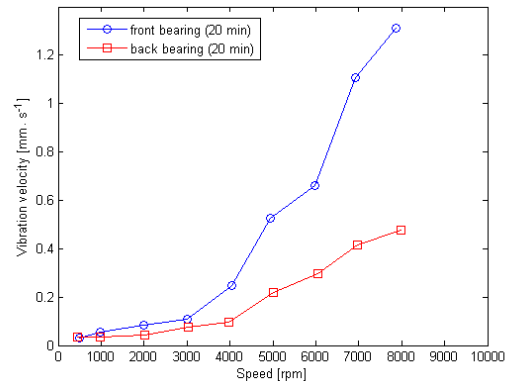


Fig. 5. Vibration velocity.

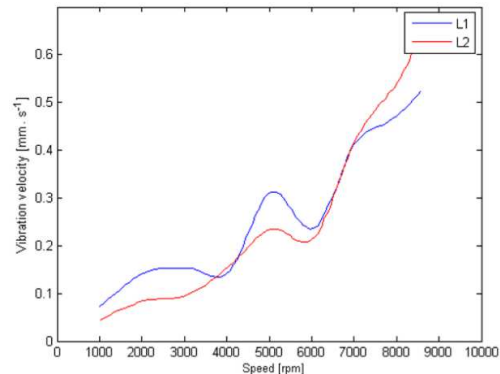


Fig. 6. Vibration velocity as function of speed ($L1$, $L2$).

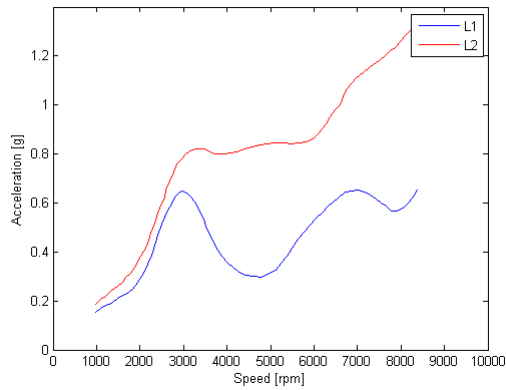


Fig. 7. Acceleration level as function of speed (L1, L2).

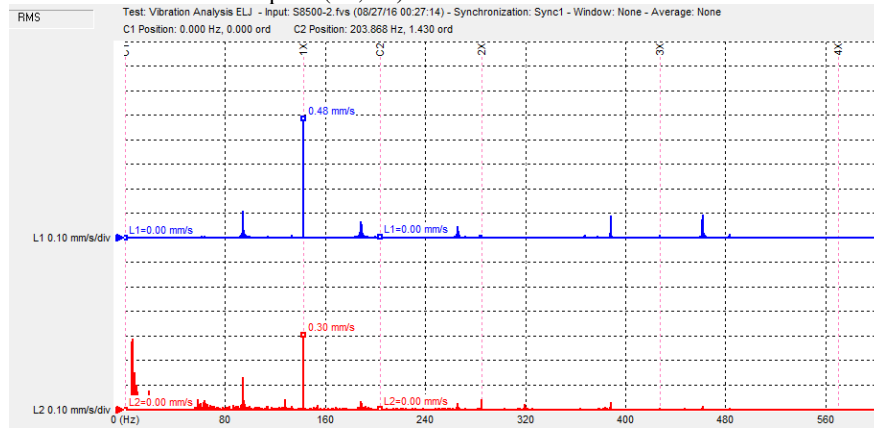


Fig. 8. Frequency spectrum at 8553 rpm.

simplified versions of spindles (not including bushes and sometimes spacers).

The main spindle bearing arrangement consists of a quadruplex combination of double back to back combination of angular contact ball bearings in the front separated by spacers, and one radial roller bearing in the rear. The front bearings are preloaded by a front nut and the back one by a rear nut. The main spindle is driven through a pulley and a belt drive Poly V form the motor.

The features of the angular contact bearings 7014 CETNH/HCP4AQBCA are: inner diameter $d = 70$ mm, outer one $D = 110$ mm, width $B = 20$ mm, number of balls $Z = 25$, and rigidity $k_{ax} = 120$ N/ μ m. The features of the cylindrical roller bearing N1012 RGT42KRCC1P4 are: inner diameter $d = 60$ mm, outer diameter $D = 95$ mm, width $B = 18$ m, number of balls $Z = 20$, and rigidity $k_{rad} = 680$ N/ μ m.

3. MODELLING AND SIMULATION

3.1 Main spindle system model

Two variants of the spindle construction were used. The first one was without cooling and therefore without cooling circuit inside housing (Fig. 9) and the second one having a water cooling circuit (Fig. 10). The simulations were performed on the assembly with all the subcomponents, unlike most of the works in the field where the simulations are done on

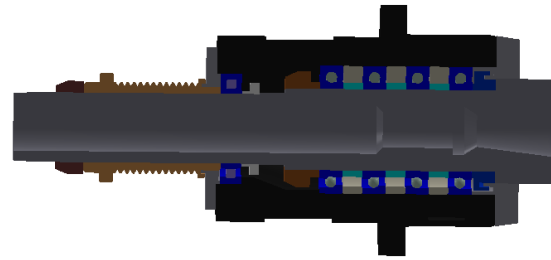


Fig. 9. Spindle bearing without cooling (cross section).

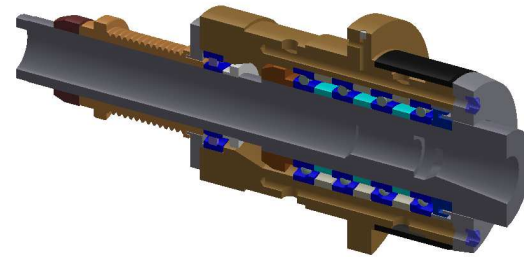


Fig. 10. Spindle bearing with water cooling system in cross section.

3.2 Main spindle thermal simulation

The distribution of temperature for spindle bearing without cooling is simulated in the case of maximum speed of 4000 rpm, after 120 min of running. Three points are measured, in the same locations as in the experimental approach for the assessment of the model accuracy: 30°C in the location of front bearing, 35°C in the location of rear bearing and 33°C in the area of belt drive Poly V.

Under these conditions, the highest temperatures are found in the rear bearing area (35°C), and in the front bearing area the temperature is on average 30°C. A higher load can be observed on the rear bearing supporting a larger force reaction caused by the belt tensioner preloading. A uniformity of the temperatures on geometric areas is observed, the materials used having a better conductivity (Figs. 11 and 12).

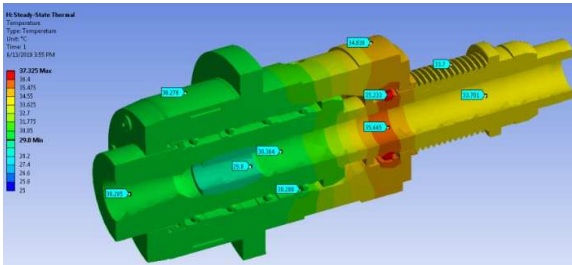


Fig. 11. Temperature distribution for spindle bearing without cooling liquid for speeds up to 4000 rpm.

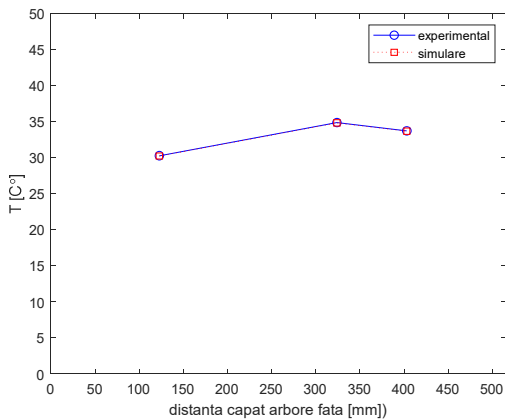


Fig. 12. Temperature distribution for spindle bearing without cooling liquid for speeds up to 4000 rpm, experimental and simulation values.

The distribution of temperature for spindle bearing with cooling liquid is simulated in the case of at maximum speed of 8500 rpm, starting

from 4500 rpm and rising it gradually during 180 min. Temperatures measured in the three points, both in experimental and simulation situations, are of 29°C in the location of the front bearing, of 30°C in the location of the rear bearing, and of 33°C in the area of the belt drive Poly V (Figs. 13–14). The same conclusion can be drawn as in the case of spindle bearing without cooling. The temperatures in the rear bearing area is of 46°C, and in the front bearing area is of 36°C.

Comparing the two situations, without cooling and with cooling, we can conclude:

- In the first case, the shaft is heated more in the rear bearing area (35°C), but this area is reduced in size, so that it does not significantly influence its expansion. Thus, the heating is uniform, the temperature of the zone for fixing the tool holder is of 30°C.
- In the second case, even if the main spindle is cooled through the housing, the temperature of the spindle is higher, but more evenly distributed. In the fixing area of the tool

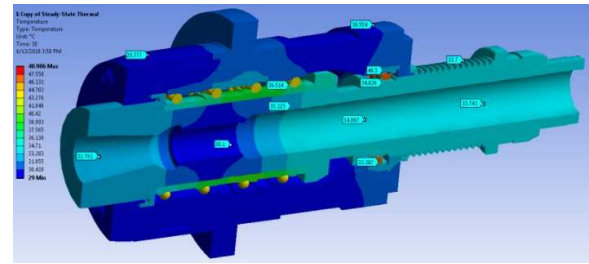


Fig. 13. Distribution of temperature for spindle bearing with cooling liquid for speeds up to 8500 rpm.

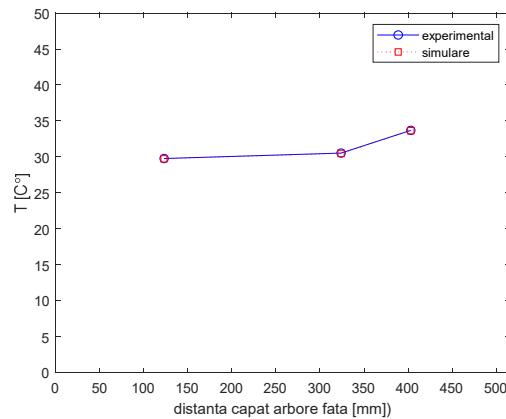


Fig. 14. Temperature distribution for spindle bearing with cooling liquid for speeds up to 8500 rpm, experimental and simulation values.

holder, the temperature is of 33°C. The cooling system contributes to a more efficient cooling of the main spindle housing, which

takes over most of the heat released by bearings and belt drive.

The cooling system is very efficient, although it is geometrically complicated and creates some turbulence, as seen from the study of the coolant flow (Fig. 15). This cooling system of the main spindle bearings also has the role of cooling the tool, in which case a more complex filtering and cooling system is required.

The output section of the liquid is much under-sized compared to the rest of the cooling channels, which leads to an increase in the fluid velocity in that area.

The main conclusions of the analysis of the behavior of the main shaft in the thermal field are:

- the necessity of resizing the rear bearing of the main spindle, this being the main source of heating;

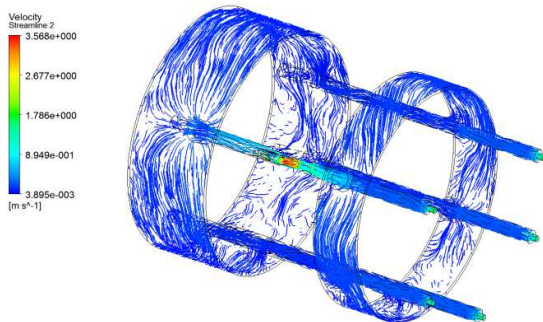


Fig. 15. Circulation of the liquid through the cooling system (speed distribution).

- a new constructive solution for releasing the rear end of the main shaft of the forces in the belt drive should be used.

3.3 Transient analysis

The transient analysis is performed under the same loading conditions as in the previous cases.

The results of these analyzes provide information on the deformations of the structures caused by the heat produced in the bearings and the belt transmission. The analysis is performed on the shaft without cooling, operating up to a speed of 4 500 rpm (Figs. 16 and 17).

A predominantly axial displacement is observed, the maximum value of 11 μm being calculated in the rear area of the main shaft. As a result of these analyzes, it is found that the front bearing is sufficiently rigid and the thermal stresses do not induce deformation in this area (especially in the area of the tool holder clamping the deformations are below 1 μm). Even if the values of deformations are higher, the accuracy of the shaft is not affected.

The stresses induced by the thermal effects are reduced, their maximum value (equivalent stress calculated according to the Von Mises criterion) being of 159 MPa in the rear bearing area. These values are lower than the permissible stresses of the materials used.

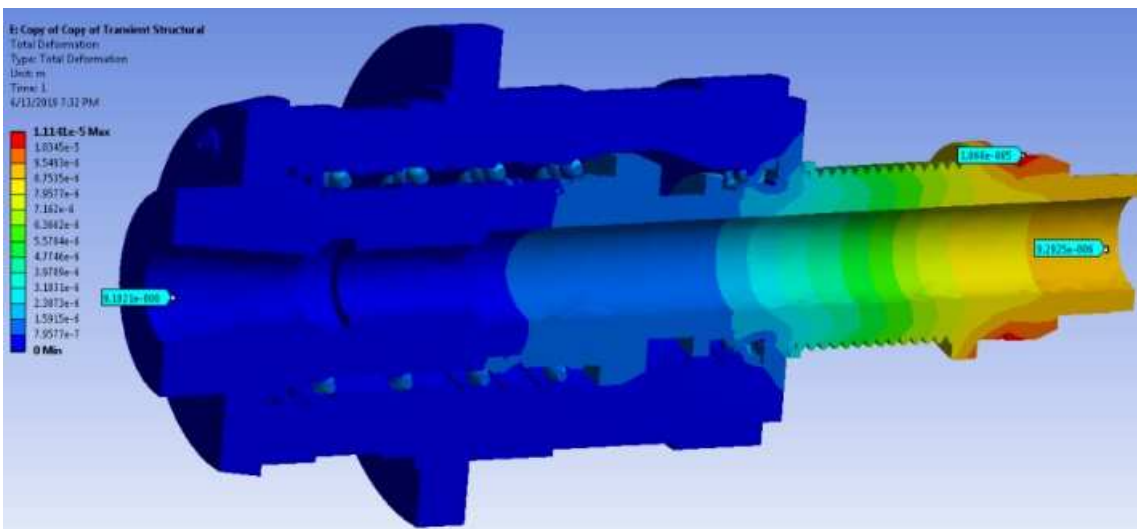


Fig. 16. Thermal deformations for shaft without cooling.

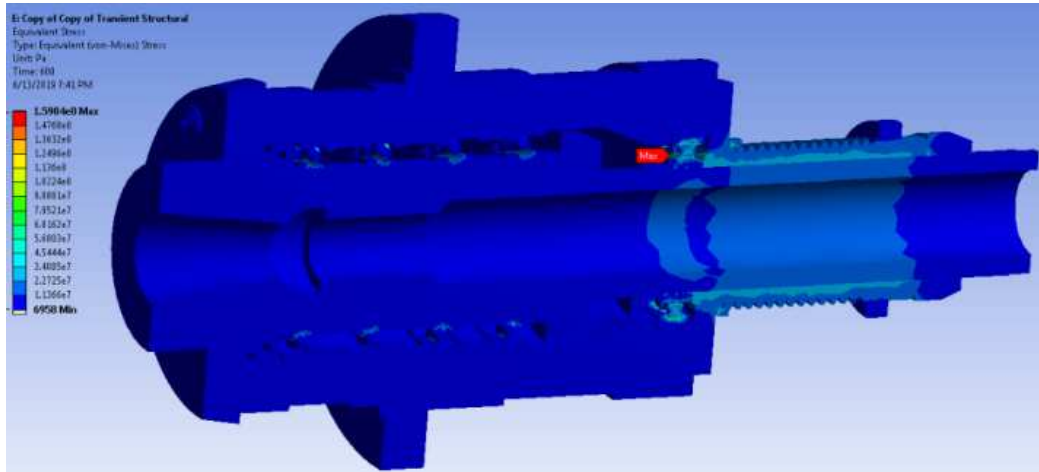


Fig. 17. The distribution of the equivalent stresses induced by the thermal effects for the shaft without cooling.

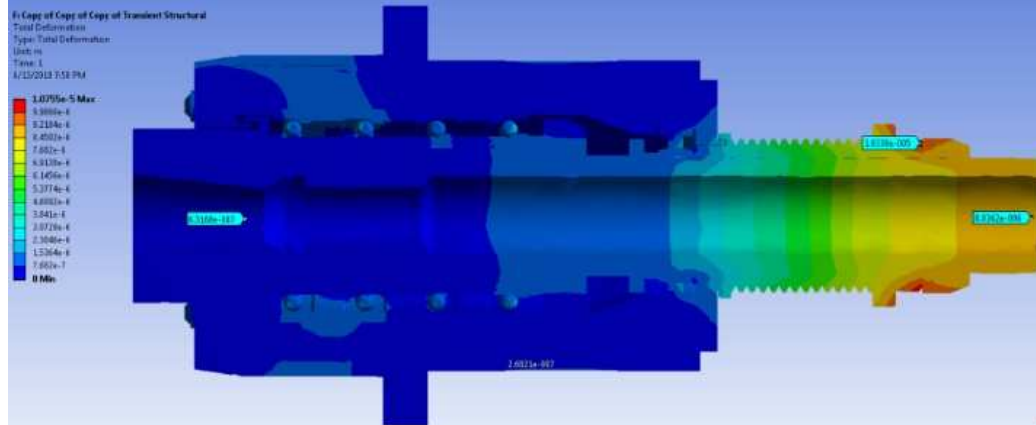


Fig. 18. Main spindle deformations under thermal effect with cooling.

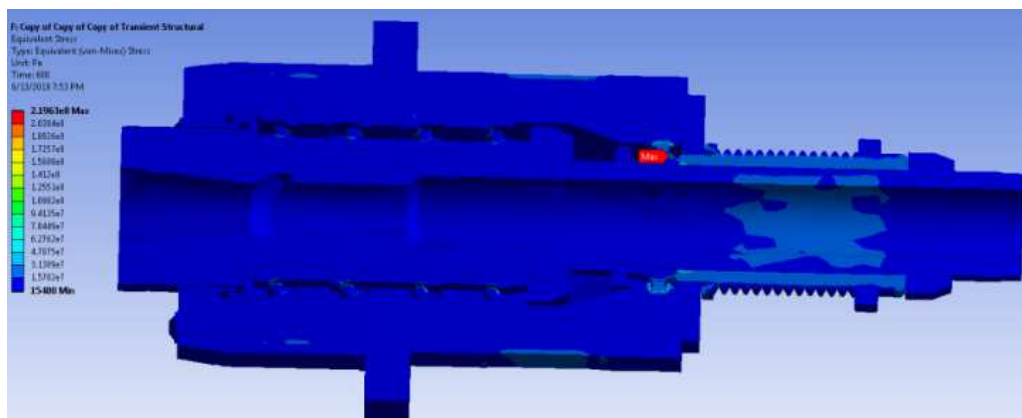


Fig. 19. Equivalent stress distribution due to the thermal effect.

The transient analysis for spindle bearing with cooling liquid is shown in Figs. 18 and 19, under the same loading conditions as in the previous cases.

Also in this model, the deformations are axial, the largest being also in the rear area, the maximum calculated value being of 10.7 μm .

The calculated equivalent stress have a maximum value of 219 MPa, lower than the permissible stresses of the materials used. However, these levels of stress combined with the effect of other loads (static or dynamic) have to be carefully analyzed, because by

compounding the effects, they could lead to deterioration of some assembly components.

The modal analysis is of interest for determining the natural frequencies of the assembly and the associated mode shapes. It can be noted that the first natural frequency has the value of $f_1 = 1750$ Hz, much higher than the rotational frequency $f_{\max} = 143$ Hz corresponding to the maximum speed of 8500 rpm (Fig. 20).

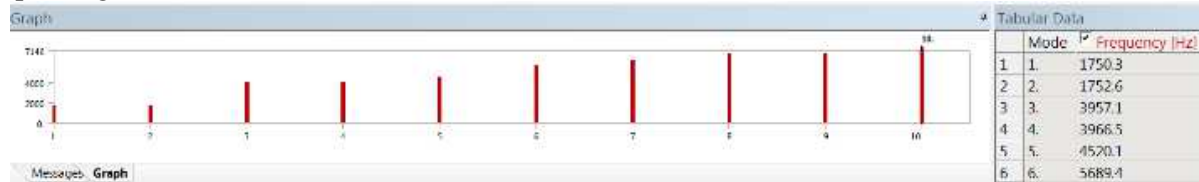


Fig. 20. Natural frequencies.

main contributions of the article are the following:

- establishing the methodology used for numerically determining the thermal variables of a shaft-bearings system driven by an electric motor through a belt.
- experimental tests were made on the real system of the main spindle mounted on the machine tool regarding the thermal behavior in idle operation and in both situations – without cooling and with cooling covering the spindle speed range of 1000–8500 rpm; dynamic measurements regarding vibration velocities, level of acceleration and frequency spectrum at 8553 rpm were performed;
- generating the CAD model of the real spindle-bearings system including the cooling circuit
- FE thermal analysis of the heat dissipated in the system by the heat generated in bearings and belt assembly an electric motor without cooling up to 4000 rpm and with cooling in the range of 4000–8500 rpm as in the case of experimental tests.
- fluid flow through the cooling circuit was simulated, some qualitative and quantitative aspects of functionality being emphasized.
- transient analysis to supply values of the deformations of the structures under the influence of the heat caused by the bearings and the belt transmission.

4. CONCLUSION

The paper had an approach on the level of CAD modeling and thermo-mechanical FEA of a main spindle-bearings assembly also subject of experimental measurements. The mathematical modeling of the heat generated in bearings is the basis for thermal loading of the FE model. The

Experimental data measured during the experimental tests were compared to those obtained by thermal analysis with ANSYS. The validation of the FE model was done by comparing the measured temperatures with those supplied by simulation for the considered points.

Simulations achieved considering non cooling along with the cooling of the housing showed errors between model and real main spindle of at most 0.2×10^{-1} . Simulations were performed for modal analysis. Experimental data were extracted regarding the frequency spectrum at the speed of 8553 rpm and the vibration and acceleration parameters at the speed of 8553 rpm.

In terms of the main spindle natural frequencies, these are much higher than those of the shaft rotational frequencies, being avoided the phenomenon of resonance.

5. REFERENCES

- [1] Constantin, G., Chapter: *Virtual în concepția și exploatarea de mașini-unelte și sisteme de mașini*, in *Modelare-Simulare-Proiectare în domeniul mașinilor-unelte și sistemelor de mașini (Virtual in design and operation of machine tools and machine systems*, in *Modeling-simulation-design in machine tools and machine systems*), Ed. Constantin, G., Printech Publishing House, Bucharest, pp. 9–79, 2014.

- [2] Altintas, Y., Brecher, C., Weck, M., & Witt, S., *Virtual machine tool*, CIRP Annals-Manufacturing Technology, 54(2), pp. 115–138, 2005.
- [3] Lin, C. W., Lin, Y. K., & Chu, C. H., *Dynamic models and design of spindle-bearing systems of machine tools: A review*, International journal of precision engineering and manufacturing, 14(3), 513–521, 2013.
- [4] Jiang, S. and Mao, H., *Investigation of Variable Optimum Preload for a Machine Tool Spindle*, International Journal of Machine Tools and Manufacture, Vol. 50, No. 1, pp. 19–28, 2010.
- [5] Kim, S. M. and Lee, S. K., *Prediction of Thermo-Elastic Behavior in a Spindle-Bearing System Considering Bearing Surroundings*, International Journal of Machine Tools and Manufacture, Vol. 41, No. 6, pp. 809–831, 2001.
- [6] Lin, C. W., Tu, J. F., and Kamman, J., *An Integrated Thermo-Mechanical-Dynamic Model to Characterize Motorized Machine Tool Spindles During Very High Speed Rotation*, International Journal of Machine Tools and Manufacture, Vol. 43, No. 10, pp. 1035–1050, 2003.
- [7] Altintas, Y. and Cao, Y., *Virtual Design and Optimization of Machine Tool Spindles*, CIRP Annals-Manufacturing Technology, 54, 379–382, 2005.
- [8] Friswell, M. I., Penny, J. E., Garvey, S.D., & Lees, A.W., *Dynamics of rotating machines*, Cambridge University Press, 2010.
- [9] Tiwari, R., *Rotor systems: analysis and identification*, CRC Press, 2017.
- [10] Harris T. A., *Rolling bearing analysis*, Wiley, 2001.
- [11] Genta, G., *Vibration of Structures and Machines*, 3rd edition, Springer, 1999.
- [12] Bossmanns, B., *Thermo-Mechanical Modeling of Motorized Spindle Systems for High Speed Milling*, PhD. Dissertation, Purdue University, 1997.
- [13] Bossmanns, B., and Tu, J. F., *A power flow model for high speed motorized spindles – heat generation characterization*, J. Manuf. Sci. Eng., 123(3), pp. 494–505, 2000.
- [14] Hongqi Li, Yung C. Shin, *Integrated Dynamic Thermo-Mechanical Modeling of High Speed Spindles, Part 1: Model Development*, Journal of Manufacturing Science and Engineering 126(1), pp. 148–157, 2004.
- [15] Hongqi Li, Yung C. Shin, *Integrated Dynamic Thermo-Mechanical Modeling of High Speed Spindles, Part 2: Solution Procedure and Validations*, Journal of Manufacturing Science and Engineering 126(1), pp.159–168, 2004.
- [16] Jorgensen, B. R., and Shin, Y. C., *Dynamics of machine tool spindle/bearing systems under thermal growth*, Journal of Tribology, 119(4), pp. 875–882, 1997.
- [17] Jedrzejewski, J., and W. Kwasny, *Modelling of angular contact ball bearings and axial displacements for high-speed spindles*, CIRP annals, 59(1), pp. 377–382, 2010.
- [18] Uhlmann, E. and Hu, J., *Thermal modelling of a high speed motor spindle*, Procedia CIRP, 1, pp. 313–318, 2012.
- [19] Liu, D., Zhang, H., Tao, Z., and Su, Y., *Finite element analysis of high-speed motorized spindle based on ANSYS*, The Open Mechanical Engineering Journal, 5(1), 2011.
- [20] Hung, J. P., Lai, Y. L., Luo, T. L., & Su, H. C., *Analysis of the machining stability of a milling machine considering the effect of machine frame structure and spindle bearings: experimental and finite element approaches*, The International Journal of Advanced Manufacturing Technology, 68(9-12), pp. 2393–2405, 2013.
- [21] Holkup, T., Cao, H., Kolář, P., Altintas, Y., and Zelený, J., *Thermo-mechanical model of spindles*, CIRP annals, 59(1), pp. 365–368, 2010.
- [22] Than, V. T., and Huang, J. H., *Nonlinear thermal effects on high-speed spindle bearings subjected to preload*, Tribology International, 96, pp. 361–372. 2016.
- [23] Brecher, C., Shneor, Y., Neus, S., Bakarinow, K., and Fey, M., *Thermal behavior of externally driven spindle: Experimental study and modelling*, Engineering, 7(02), pp. 73–92, 2015.
- [24] Zheng, D., and Chen, W., *Thermal performances on angular contact ball bearing of high-speed spindle considering structural constraints under oil-air lubrication*, Tribology International, 109, pp. 593–601, 2017.
- [25] Nakajima, K., *Thermal contact resistance between balls and rings of a bearing under axial, radial, and combined loads*, Journal of thermophysics and heat transfer, 9(1), pp. 88–95, 1995.
- [26] Cao, Y., and Altintas, Y., *A general method for the modeling of spindle-bearing systems*, Journal of mechanical design, 126(6), pp. 1089–1104, 2004.

- [27] Antoine, J-F., G. Abba, and A. Molinari, *A new proposal for explicit angle calculation in angular contact ball bearing*, pp. 468–478, 2005.
- [28] Jin, C., Wu, B., and Hu, Y., *Heat generation modeling of ball bearing based on internal load distribution*, *Tribology International*, 45(1), pp. 8–15, 2012.
- [29] Kim, J. D., Zverv, I., and Lee, K. B., *Thermal model of high-speed spindle units*, *Intelligent Information Management*, 2(05), pp. 306–315, 2010.

Analiza termo-mecanică complexă a arborilor principali acționați din exterior – studiu de caz

Rezumat: *Articolul tratează din perspectiva modelării complexe ansamblul arbore principal-rulmenți care funcționează la turații mari. Se are în vedere simularea comportarea dinamică și termomecanică. Sunt evidențiate câteva contribuții importante în ceea ce privește simularea complexă a arborelui principal. Se tratează modelarea matematică a generării căldurii în rulmenții radial-axiali cu bile cu contact unghiular. Căldura generată se consideră sursa din modelele FEM. Articolul abordează un studiu de caz al arborelui principal al unui centru de prelucrare prin frezare cu turații de până la 9000 rpm. Sunt obținute rezultatele experimentale privind temperaturile lagărelor pentru diferite viteze cu și fără răcirea carcasei și, de asemenea, unele măsurători dinamice. Se generează modelul CAD al arborelui principal studiat care apoi este importat în programul cu elemente finite. Pe baza modelului matematic al căldurii, modelul este încărcat cu sursele de căldură din rulmenți și transmisia prin curele și, în urma simulării, se obține distribuția de temperatură. Sunt luate în considerare situațiile fără răcire (până la 4000 rpm) și cu răcire pentru 4000-8500 rpm. Valorile simulate aproape că se suprapun cu cele măsurate, astfel încât modelul este validat. Se obțin prin simulare deformațiile termice pentru ansamblul cu răcire și fără răcire. Frecvențele naturale sunt obținute prin simulare dinamică și comparate cu cele din funcționare. Concluziile pun în evidență un algoritm pentru cercetare experimentală combinat cu o modelare matematică și o analiza numerică prin FEA și aspecte specifice legate de funcționalitatea ansamblului.*

George CONSTANTIN, Prof., PhD, University "Politehnica" of Bucharest, Robots and Manufacturing Systems Department, george.constantin@icmas.eu, Splaiul Independenței 313, district 6, 060042, Bucharest, Romania, Tel: 0040 21 402 9174.

Constantin DOGARIU, Prof., PhD, University "Politehnica" of Bucharest, Robots and Manufacturing Systems Department, cdogariu@gmail.com, Splaiul Independenței 313, district 6, 060042, Bucharest, Romania, Tel: 0040 21 402 9174.

Claudiu-Florinel BÎȘU, Assoc. Prof., PhD, University "Politehnica" of Bucharest, Robots and Manufacturing Systems Department, cfbisu@gmail.com, Splaiul Independenței 313, district 6, 060042, Bucharest, Romania, Tel: 0040 21 402 9174.

Andrei GHEORGHITĂ, PhD Student, University "Politehnica" of Bucharest, Robots and Manufacturing Systems Department, andu_ghe@yahoo.com, Splaiul Independenței 313, district 6, 060042, Bucharest, Romania, Tel: 0040 21 402 9174.

Dragoș AROTĂRIȚEI, Prof., PhD, University of Medicine and Pharmacy "Grigore T Popa", Str. University str 16, Iasi, Romania, Tel: 0040 232 213 573.

Gabriel Ionuț GHIONEA, Assoc. Prof., PhD, University "Politehnica" of Bucharest, Manufacturing Engineering Department, ionut76@hotmail.com, Splaiul Independenței 313, district 6, 060042, Bucharest, Romania, Tel: 0040 021 402 9373.